Binding-Site Determination from Angle-Resolved Ultraviolet Photoemission Intensity Modulations—Classification of Initial States into Two Types

C. H. Li and S. Y. Tong
Surface Studies Laboratory and Department of Physics, University of Wisconsin, Milwaukee, Wisconsin 53201

(Received 29 December 1978)

The emission spectra from a given adatom initial state are analyzed as a function of photon energy. We can classify the emission spectra into two classes according to the initial state. For initial states with no nodes, the emission spectra contain interference modulations sensitive to the adsorbate-substrate distance. For initial states with nodes, the spectra at low energies are dominated by a main peak which is independent of surface structure and which has its origin in the emission of a single adatom.

In an earlier paper, we calculated the emission spectra from a given initial state of an adsorbate atom as a function of photon energy.[1] We found that for certain initial states, the emission intensities contain measurable interference modulations. The positions of peaks and valleys of the modulations are sensitively related to the adsorbate-substrate layer separation distance. We indicated that this is an important mode of measurement for angle-resolved ultraviolet photoemission spectroscopy (UPS) because the interference modulations may be utilized to determine binding sites of adsorbed species. This potential use of an angle-resolved UPS was realized by the experiments of Kevan *et al.*,[2] who measured the modulations in the emission spectra from the 3*d* core levels of Ni(001)-*c*(2×2)Se and -*p*(2×2)Se. More recent experiments on another system[3] confirm our contention that the interference modulations are common features in many overlayer systems.

In further studies of emission spectra from other initial states, we found spectral results which behave very differently. There is a class of initial states from which the emission spectra contain a single main peak. We traced this peak to an atomiclike emission of the adatom. For this class of initial states, the emission spectra at low energies are dominated by this main peak. The mean position of this peak is relatively insensitive to the adsorbate-substrate spacing.

We group the emission spectra into two types, according to the initial state of the photoexcited electron. In one group, there are intensity modulations which can be used to study surface binding positions. In the other, the main feature is a single peak arising from atomiclike emission. In the following, we present evidence in support of this classification and give rules of thumb to separate initial states into the two types.

We first present the intensity spectra, for emission normal to the surface, from the 3*d* core level of Se overlayers on Ni(001). The calculated spectra for both *c*(2×2) (Ref. 1) and *p*(2×2) ordered overlayers showed interference modulations in an extended energy range. Kevan *et al.* measured this emission for Ni(001)-*c*(2×2)Se and -*p*(2×2)Se and found the interference modulations.[2] In Fig. 1, the comparison between theory and experiment is shown for Ni(001)-*p*(2×2)Se. In the theory, the Se atom is placed at the hollow site with an adsorbate-substrate separation $d_\perp = 1.55$ Å (the value determined by low-energy electron diffraction[4]) and with $d_\perp = 1.95$ Å. We also show the theoretical curve for Se at the top site with $d_\perp = 2.34$ Å. The agreement between theory and experiment for the hollow-site, $d_\perp = 1.55$ Å case is excellent, especially above 60 eV. The calculated peak positions are very sensitive to the value of $d_\perp$, e.g., the peak at kinetic energy

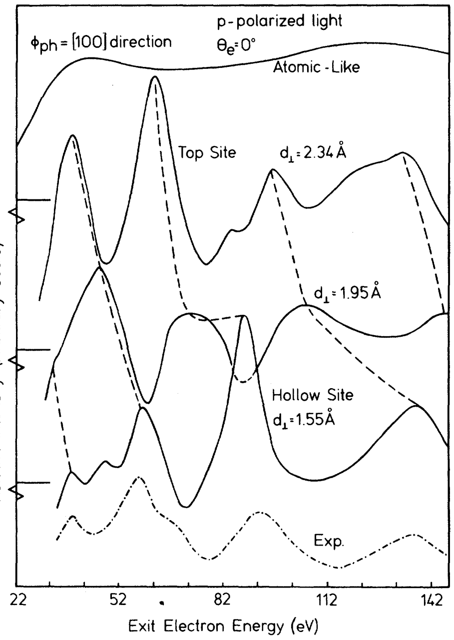

FIG. 1. Intensity modulations for emissions from 3*d* level of Ni(001)-*p*(2×2)Se, $\theta_{ph} = 60°$.

© 1979 The American Physical Society

$E_k = 90$ eV moves to 72 eV as $d_\perp$ varies from 1.55 to 1.95 Å. Similarly, the peak at $E_k = 138$ eV moves to 103 eV for the same change in $d_\perp$. The spacing $d_\perp = 1.95$ Å corresponds approximately to the layer distance for a bridge-bonded Se overlayer. With such sensitivity is is clear that the intensity modulations can be used to distinguish between adsorption sites. In Fig. 1, the calculated 3*d* emission from atomic Se is also shown. The atomic emission is calculated by including scattering of the outgoing electron off a single Se potential only. The Se potential is formed by overlapping an atomic Se potential with the nearest-neighbor Ni potentials. The atomic spectrum is a smooth function of energy, with a rise at 40 eV.

The peak positions of the modulations are insensitive to the choice of the scattering potentials. In Fig. 2, we show calculations from three types of potentials[5]: (i) bulk band-structure potential, (ii) $X\alpha$ scattered-wave cluster potential, and (iii) $X\alpha$ cluster potential with a positive hole at the host atom [curves *a*, *b*, and *c*, respectively, in Fig. 2]. Above 60 eV, the three schemes agree very well with each other and with the experiment. Shifts in peak positions, due to phase-shift differences, of less than 2.5 eV are present. But small shifts of this magnitude are noncritical in view of the much larger movements of peak positions as $d_\perp$ is changed. The relative intensities of peaks depend on the rise in intensity of the atomiclike emission curve (shown at 40 eV in Fig. 1). This in turn depends on the transition matrix elements. The position of the rise could be model dependent.[6] Thus one should not rely too heavily on relative intensities at the low-energy end (below $E_k = 60$ eV) in using these modulations for structural analysis.

The emission from the 4*d* core level of $c(2\times2)$Te on Ni(001) is shown in Fig. 3. Here we found the spectra distinctly different from those of Se overlayers. There is only a main peak, with small modulations on this peak and modulations at higher energies. The main peak remains at about the same location when we vary the Te-Ni layer spacing from $d_\perp = 1.90$ to 2.30 Å. A similar peak is seen in the emission spectra of atomic Te (top curve, Fig. 3). The absolute value of the $c(2\times2)$Te peak (normalized to the same coverage) is about 6 times larger and the valley-to-peak height is 10 times larger than corresponding quantities in the Se modulations.

The normal emission from the 2*p* core level of Ni(001)-$c(2\times2)$Na is shown in Fig. 4. Here, as in the Se case, intensity modulations are found in an extended energy range. These modulations have been recently measured in the experiments of Williams *et al.*[3] The emission spectrum from atomic Na is again a smooth curve, with a rise at about 30 eV.

Thus, there are two classes of emission spectra. Their origin must come from the initial or-

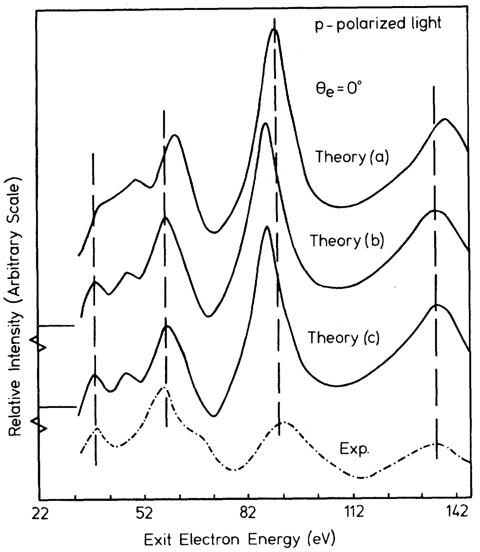

FIG. 2. Three potential models for 3*d* emissions of Ni(001)-$p(2\times2)$Se; $\theta_{\text{ph}} = 60°$, $\varphi_{\text{ph}} =$ [100] direction.

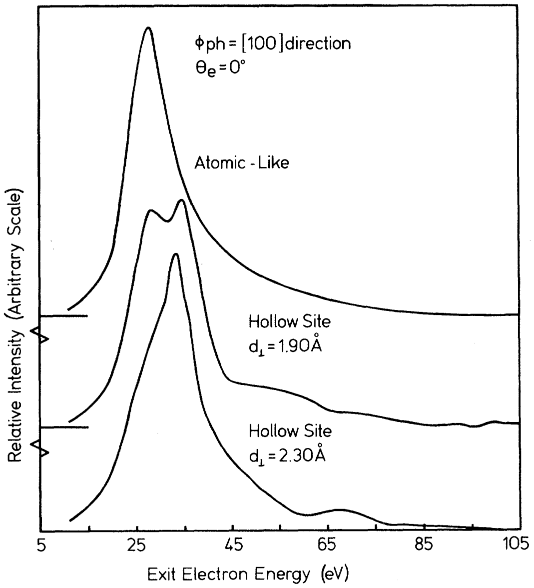

FIG. 3. Emission spectra for 4*d* level of Ni(001)-$c(2\times2)$Te; $\theta_{\text{ph}} = 47.7°$; *p*-polarized light.

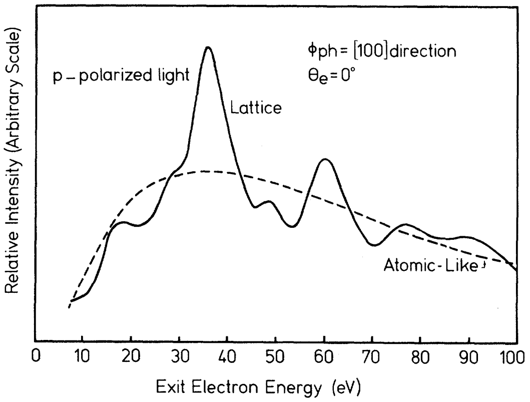

FIG. 4. Intensity modulations for emissions from $2p$ level of Ni(001)-$c(2\times 2)$Na; $\theta_{\text{ph}}=47.7°$.

bitals. It is known from gas-phase experiments and calculations[7] that the radial function R_{nl} of an initial state with $n=l+1$ is nodeless. The nodeless initial orbital gives rise to a smooth atomic emission cross section. When emitted from an adsorbate atom, multiple scatterings of the final-state electron between adsorbate and substrate layers produce the observed modulations. An initial state with radial function R_{nl} with $n\neq l+1$ contains one or more nodes. The atomic emission contains a main peak, decreasing to a Cooper minimum[7] at higher energies. Final-state scatterings produce modulations small compared to the valley-to-peak height of this main peak. This atomic emission dominates the spectra for $E_k \leq 60$ eV.

Thus, we have a simple classification scheme: To study surface geometry, one should probe initial levels with no nodes, i.e., $1s$, $2p$, $3d$, $4f$, etc., orbitals. On the other hand, if one probes initial states with nodes, one measures mainly atomic emission properties, unless E_k is well above the atomic peak.

If one probes initial orbitals with nodes to study surface geometry, it is possible to obtain intensity modulations due to final-state scatterings by dividing out the atomic emission cross section. However, the peak of calculated atomic cross section (shown at 26 eV in Fig. 3) could be model dependent. Thus the quotients near the peak are unreliable. Or, one may use measured atomic photoemission cross sections from gas-phase data. But gas-phase atomic cross sections are not always directly comparable to those of an adsorbed atom. Thus it is best to avoid energies near the atomic peak and to concentrate on higher-energy data. To obtain enough signal, one should go to kinetic energies about 50 eV above the Cooper minimum.

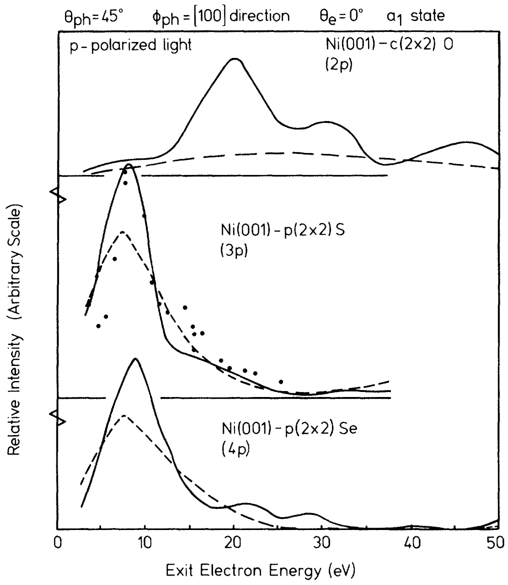

FIG. 5. Emission spectra from valence levels of chalcogens. Solid curves, emissions from ordered overlayers; broken curves, emissions from atoms; and dots, experiment.

Using this scheme, we look at emissions from valence orbitals: $2p$, $3p$, and $4p$ levels of chalcogens O, S, and Se on Ni(001). If the above classification also holds true for valence-level emissions, we would expect the nodes in $3p$ and $4p$ orbitals of S and Se to produce main peaks in both the atomic and overlayer spectra. Such were found to be the case (Fig. 5). The data for the S overlayer were measured by Plummer *et al.*[8,9]

For oxygen, the atomic emission is smooth because of the nodeless $2p$ level. Final-state scatterings produce modulations with a main peak at $E_k=20$ eV (Fig. 5). Comparing the O, S, and Se systems, we note that the O peak at $E_k=20$ eV is sensitive to the O-Ni spacing while the S and Se peaks at $E_k=8.0$ and 9.0 eV, respectively, are not sensitive to the S-Ni and Se-Ni spacings.

We now compare the modulations found here with those of surface extended x-ray–absorption fine structure (SEXAFS). The modulations share a common origin, i.e., final-state scatterings. In SEXAFS, a spherical average is taken and the surface parameter extracted is the nearest-neighbor distance. However, the nearest-neighbor distance alone does not fix the atomic position. For that, we need either the next-nearest-neighbor distance or the coordination number at the adsorption site. Both of these are difficult to determine accurately in SEXAFS. For the angle-resolved UPS modulations discussed here, the emissions are measured at fixed final directions $\vec{k}_f$. This directional dependence results in the determination of $d_\perp$, the adsorbate-substrate layer separation distance. In common cases, knowledge of this distance also fixes the chemisorption position.

This work is supported by National Science Foundation Grant No. DMR 77-28112 and the University of Wisconsin–Milwaukee Graduate School.

---

[1] C. H. Li and S. Y. Tong, Phys. Rev. B (to be published).

[2] S. D. Kevan, D. H. Rosenblatt, D. Denley, B.-C. Lu, and D. A. Shirley, Phys. Rev. Lett. 41, 1565 (1978).

[3] G. P. Williams, F. Cerrina, I. T. McGovern, and G. J. Lapeyre, to be published.

[4] M. Van Hove and S. Y. Tong, J. Vac. Sci. Technol. 12, 230 (1975).

[5] C. H. Li and S. Y. Tong, to be published.

[6] U. Fano and J. W. Cooper, Rev. Mod. Phys. 40, 441 (1968).

[7] J. W. Cooper, Phys. Rev. 128, 681 (1962).

[8] E. W. Plummer, B. P. Tonner, N. Holzwarth, and A. Liebsch, to be published.

[9] For a valence orbital, this classification is valid only if the orbital retains a strong atomic nature.

Spin Polarization of Liquid ^{3}He by Rapid Melting of Polarized Solid

M. Chapellier,[a] G. Frossati,[b] and F. B. Rasmussen
Physics Laboratory I, H. C. Ørsted Institute, DK-2100 Copenhagen, Denmark

(Received 1 February 1979)

In liquid ^{3}He in a Pomeranchuk cell, spin polarizations of 5–20% have been obtained. The method involved production of polarized solid by Pomeranchuk cooling in magnetic fields from 0.03 to 3 T, followed by rapid decompression to a pressure between 2.9 and 0.2 MPa. Relaxation times in the liquid range from 1 to 5 min, increasing with decreasing pressure and with increasing field.

At low temperatures, the paramagnetic susceptibility of liquid ^{3}He tends towards a constant value because of Fermi statistics. Interactions in the liquid cause the experimentally observed limiting susceptibility[1] to be substantially higher than for an ideal gas of fermions, the enhancement factor being as high as 24 at pressures near solidification. These interactions are not yet understood. In spite of the susceptibility enhancement, spin polarization in the liquid remains small under conditions of thermal equilibrium. A field of 2.3 T is just sufficient to produce 1% polarization at the lowest temperatures and near the solidification pressure. Studies of nuclear orientation in liquid ^{3}He offer very interesting prospects, however. Among the effects of a high spin polarization predicted in recent papers by Castaing and Nozières,[2] and by Lhuillier and Laloë,[3] is a reduction of the melting pressure at low temperatures, leading eventually to a complete disappearance of the melting curve minimum near full polarization. Castaing and Nozières note that the reduction in melting pressure might tell whether the liquid owes its enhanced susceptibility to the proximity of a ferromagnetic instability. In that case the melting pressure should be suppressed below the vapor pressure, causing one or two triple points to appear in the phase diagram. The reduced melting pressure would allow studies of solid ^{3}He at lower pressures than ever before, thus increasing chances for observing the vacancy solid phase, envisaged by Andreev and Lifshitz.[4]

As a first experimental step into this field of research we have followed the suggestion of Castaing and Nozières to produce polarized liquid by melting of solid ^{3}He that has been previously polarized in a magnetic field applied at low temperature. Although the relaxation time in the polarized liquid was estimated to be some minutes, it was not clear from the outset, that polarization would survive during the time interval of melting where additional relaxation processes may be effective.

Our ^{3}He sample (^{4}He content less than 1000 ppm) was contained in the cylindrical plastic Pomeranchuk cell shown in Fig. 1. Construction details of this type of cell have been given previously.[5] The sample volume is approximately 0.15 cm^3. The cell was mounted inside the mix-

© 1979 The American Physical Society